Combined deficiency for MAP kinase-interacting kinase 1 and 2 (Mnk1 and Mnk2) delays tumor development

Takeshi Ueda[a], Masato Sasaki[a], Andrew J. Elia[a], Iok In Christine Chio[a,b], Koichi Hamada[c], Rikiro Fukunaga[d], and Tak W. Mak[a,b,1]

[a]The Campbell Family Institute for Breast Cancer Research, Ontario Cancer Institute, University Health Network, Toronto, ON, Canada M5G 2C1; [b]Department of Medical Biophysics, University of Toronto, Toronto, ON, Canada M5G 2C1; [c]Center for AIDS Research, Kumamoto University, 2-2-1 Honjo, Kumamoto 860-0811, Japan; and [d]Department of Medical Chemistry, Graduate School of Medicine, Kyoto University, Yoshida-Konoe, Sakyo-ku, Kyoto 606-8501, Japan

This contribution is part of the special series of Inaugural Articles by members of the National Academy of Sciences elected in 2002.

Contributed by Tak W. Mak, June 9, 2010 (sent for review March 18, 2010)

MAP kinase-interacting kinase 1 and 2 (Mnk1 and Mnk2) are protein-serine/threonine kinases that are activated by ERK or p38 and phosphorylate eIF4E, which is involved in cap-dependent translation initiation. However, Mnk1/2 double knockout (Mnk-DKO) mice show normal cell growth and development despite an absence of eIF4E phosphorylation. Here we show that the tumorigenesis occurring in the Lck-Pten mouse model (referred to here as tPten$^{-/-}$ mice) can be suppressed by the loss of Mnk1/2. Phosphorylation of eIF4E was greatly enhanced in lymphomas of parental tPten$^{-/-}$ mice compared with lymphoid tissues of wild-type mice, but was totally absent in lymphomas of tPten$^{-/-}$; Mnk-DKO mice. Notably, stable knockdown of Mnk1 in the human glioma cell line U87MG resulted in dramatically decreased tumor formation when these cells were injected into athymic *nude* mice. Our data demonstrate an oncogenic role for Mnk1/2 in tumor development, and highlight these molecules as potential anticancer drug targets that could be inactivated with minimal side effects.

eIF4E | glioma | lymphoma | mouse model

Mnk1 and Mnk2 are ubiquitously expressed protein-serine/threonine kinases that are directly activated by ERK or p38 MAP kinases (1, 2). When activated in vitro, Mnk1/2 can phosphorylate the eukaryotic translation initiation factor 4E (eIF4E) (2–5). The eIF4E protein binds to the 5′ cap structure of mRNAs and is essential for cap-dependent translational initiation (6). However, the biological functions of the Mnk kinases and the significance of Mnk-mediated eIF4E phosphorylation have been controversial because Mnk1/2 double knockout (Mnk-DKO) mice exhibit normal cell growth and development despite an absence of eIF4E phosphorylation (7).

Several lines of evidence have suggested that eIF4E can act as a bona fide oncogenic accelerator in vivo (8–12). eIF4E is overexpressed in several types of human cancers and has been linked to poor prognosis in patients with tumors (8, 11). Similarly, transgenic mice overexpressing eIF4E develop tumors in multiple organs (12). Clinical studies have indicated that not only eIF4E overexpression but also eIF4E phosphorylation may contribute to tumor progression. Enhanced eIF4E phosphorylation has been observed in various solid tumors (13) and lymphomas (14) and correlates with poor patient prognosis, particularly in non-small-cell lung cancer (15). Furthermore, Mnk1 is highly expressed in hematological malignancies (16, 17), and both Mnk1 and Mnk2 are up-regulated in solid tumors such as gliomas and ovarian cancers (18, 19). Consistent with these clinical findings, in vitro studies have shown that NIH 3T3 cells expressing phosphodefective eIF4E display diminished transformation activity, whereas overexpression of wild-type (WT) eIF4E fully transforms this cell line (20, 21). Similarly, overexpression of a constitutively active Mnk1 mutant, or a phosphomimetic eIF4E mutant, promotes c-Myc-mediated lymphomagenesis in vivo (14). Finally, recent in vitro studies indicate that Mnk1/2-mediated phosphorylation of other substrates, including Sprouty2, cPLA2, and hnRNPA1, may also influence tumorigenesis (22–25). Collectively, these in vitro and in vivo studies and clinical observations strongly suggest that an axis involving Mnk1/2 and phosphorylation of eIF4E (and perhaps other substrates) can enhance tumorigenesis.

To investigate the physiological significance of eIF4E phosphorylation in tumorigenesis, we crossed Mnk-DKO mice with tPten$^{-/-}$ mice and examined various aspects of lymphomagenesis. We report that Mnk1/2 deficiency delays tumor development in the context of T cell-specific Pten loss in vivo. Importantly, Pten-null lymphomas lacking Mnk1 and Mnk2 showed no detectable level of eIF4E phosphorylation. Furthermore, stable shRNA-mediated knockdown of Mnk1 in the human glioma cell line U87MG resulted in dramatically reduced tumorigenic activity in *nude* mice. Our results suggest that inhibition of Mnk1/2 might be an effective treatment option for some human cancers and that such agents would have minimal side effects.

Results

Mnk1/Mnk2 Double Deficiency Does Not Affect Cellular Responses to Culture Stress. To determine the role of Mnk1/2 in untransformed cells, we examined primary mouse embryonic fibroblasts (MEFs) from Mnk-DKO mice both at steady state and after exposure to various culture stresses. Primary Mnk-DKO MEFs proliferated at the same rate as control (Mnk1$^{+/-}$Mnk2$^{+/-}$) MEFs under standard culture conditions (Fig. 1*A*), and showed comparable cell growth and apoptosis under conditions of either low glutamine (Fig. 1*B*) or glucose starvation (Fig. 1*C*).

We next determined the effects of Mnk1/2 deficiency on cellular responses to hypoxia or oxidative stress. Hypoxia induces the expression of a subset of genes directly regulated by the transcription factor HIF-1α (hypoxia-inducible factor-1α). The translation of the HIF-1α mRNA is cap-dependent (26), and may be fine-tuned by Mnk1/2-mediated phosphorylation of eIF4E (27). In addition, HIF-1α mRNA contains an internal ribosomal entry site (IRES) in its 5′ untranslated region. It has been suggested that eIF4E availability may control the switch between cap-dependent and IRES-mediated translation (28, 29). However, when we measured expression levels of two major HIF-1α target genes, Glut1 (glucose transporter isoform-1) and Vegf (vascular endothelial growth factor), in WT and Mnk-DKO MEFs cultured in 0.2% oxygen, we found that these genes were induced to the same level in both genotypes (Fig. 1*D*). Similarly, WT and Mnk-DKO MEFs

Author contributions: T.U., K.H., R.F., and T.W.M. designed research; T.U., M.S., A.J.E., and I.I.C.C. performed research; T.U., M.S., A.J.E., I.I.C.C., and T.W.M. analyzed data; and T.U. and T.W.M. wrote the paper.

The authors declare no conflict of interest.

Freely available online through the PNAS open access option.

See Commentary on page 13975.

[1]To whom correspondence should be addressed. E-mail: tmak@uhnres.utoronto.ca.

This article contains supporting information online at www.pnas.org/lookup/suppl/doi:10.1073/pnas.1008136107/-/DCSupplemental.

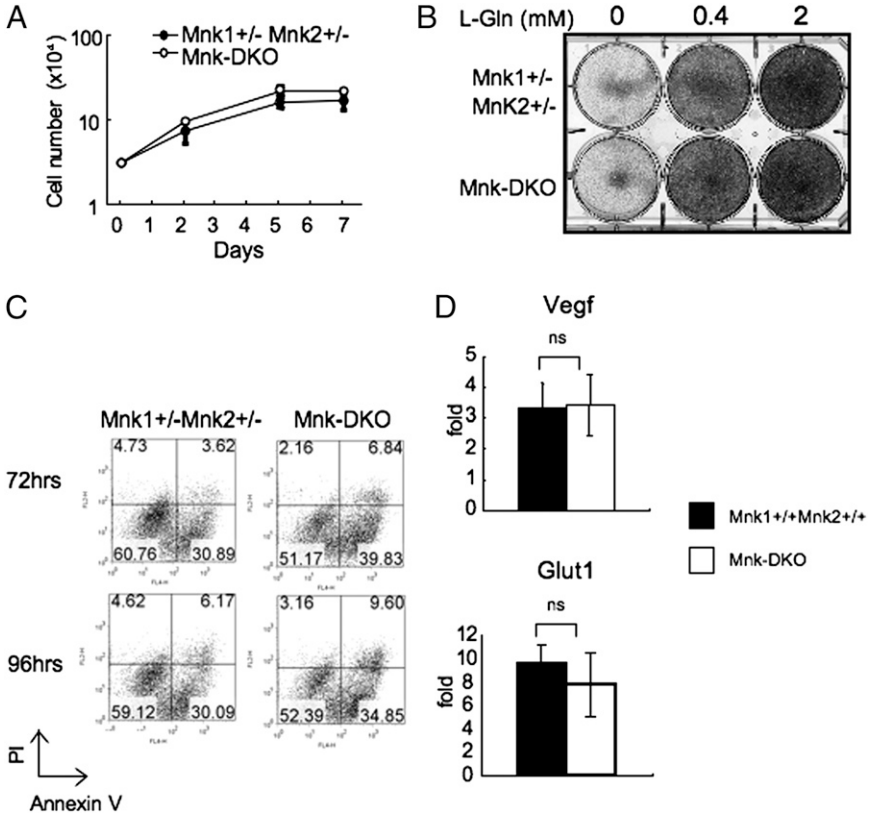

Fig. 1. Mnk1 and Mnk2 are not essential for steady-state cell growth or responses to culture stress. (*A*) Growth curves of primary MEFs of the indicated genotypes under standard culture conditions. Data shown are the mean ± SD of three cultures/genotype. (*B*) L-glutamine starvation. Primary MEFs of the indicated genotypes (1×10^5 cells/well) were cultured at the indicated concentrations of L-glutamine for 7 d and stained with 0.5% crystal violet dye in 20% ethanol. (*C*) Glucose starvation-induced apoptosis. Primary MEFs of the indicated genotypes were cultured in the absence of D-glucose for the indicated time points, stained with Annexin V/PI, and analyzed by flow cytometry. Percentages of positive cells within a quadrant are indicated. (*D*) Hypoxia. Spontaneously immortalized MEFs of the indicated genotypes were cultured in 0.2% oxygen for 24 h. The induction of Vegf and Glut1 mRNAs was measured by quantitative real-time PCR and normalized to values observed under normoxia. For all figures, results presented are representative of at least two independent trials.

treated with hydrogen peroxide (H_2O_2) accumulated equivalent levels of reactive oxygen species (ROS) (30), as detected using a CM-H_2DCFDA [5-(and-6)-chloromethyl-2′,7′-dichlorodihydrofluorescein diacetate, acetyl ester] fluorescent probe (Fig. S1). These data indicate that Mnk1/2 kinases are dispensable for cellular responses to these forms of culture stress.

Mnk1/2 Double Deficiency Inhibits Ras-Induced Transformation of Primary MEFs. It has been previously reported that Mnk1/2 kinases are involved in Ras-mediated oncogenesis in rat epithelial cells (31). To investigate the role of Mnk1/2 in the transformation of murine cells, we infected $Mnk1^{+/-}Mnk2^{+/-}$ and Mnk-DKO primary MEFs with retroviruses expressing Ras (H-RasV12) and T-Ag (SV40 large T antigen). Mnk-DKO MEFs infected with Ras and T-Ag proliferated to the same degree as infected control cells under standard culture conditions (Fig. 2*A*). However, the colonies derived from transformed Mnk-DKO MEFs in soft agar were smaller in size than colonies derived from transformed $Mnk1^{+/-}Mnk2^{+/-}$ MEFs (Fig. 2*B*). In addition, transformed Mnk-DKO MEFs generated significantly fewer ($P = 0.003$) colonies in soft agar compared with transformed $Mnk1^{+/-}Mnk2^{+/-}$ MEFs (Fig. 2*C*), suggesting that endogenous Mnk1/2 kinases can promote Ras-mediated oncogenic transformation.

Mnk1/2 Double Deficiency Leads to Delayed Tumorigenesis in a Pten-Deficient Lymphoma Model. The Pten-PI3K pathway is essential for Ras-driven cellular transformation and in vivo tumorigenesis (32), and eIF4E is a critical oncogenic effector downstream of Pten-PI3K pathway (8, 10, 12). These connections prompted us to evaluate in vivo the link between Mnk1/2 and tumorigenesis driven by loss of Pten. We compared the tumor-free survival of T-cell-specific Pten conditional knockout ($LckCrePten^{flox/flox}$, i.e., $tPten^{-/-}$) mice also lacking Mnk1 and Mnk2 ($tPten^{-/-}$; Mnk-DKO mice) with that of $Pten^{-/-}$; non-Mnk-DKO mice (including $Mnk1^{+/-}Mnk2^{+/-}$, $Mnk1^{-/-}Mnk2^{+/-}$, and $Mnk1^{+/-}Mnk2^{-/-}$ genotypes). Most $tPten^{-/-}$; non-Mnk-DKO mice (73%) exhibited signs of lymphoma at around 70 d (10 wk), with a maximal latency of 16 wk (Fig. 3*A*). This progression was in line with results previously reported for this model (33–35). Notably, $tPten^{-/-}$; Mnk-DKO mice demonstrated delayed tumor incidence with a median tumor-free survival time of 94 d ($P = 0.005$) (Fig. 3*A*), although all these mice had developed lymphomas by 18 wk. Lymphoma-containing tissues from $tPten^{-/-}$; Mnk-DKO mice also appeared smaller in size than those of control mice (Fig. 3*B*). These results suggest that endogenous Mnk1/2 kinases can enhance the tumorigenesis associated with loss of Pten in vivo.

Absence of eIF4E Phosphorylation in $tPten^{-/-}$; Mnk-DKO T-Cell Lymphomas. To characterize the tumors in $tPten^{-/-}$; Mnk-DKO mice, we used flow cytometric analyses. About 60% of the tumors in these animals could be classified as pure $CD4^+$ single positive (SP) T-cell lymphomas (Fig. 3*C*), whereas 40% were a mixture of $CD4^+$ SP and $CD4^+CD8^+$ double positive (DP) T cells. $CD8^+$ SP lymphomas were never observed, consistent with a previous report (35). In $tPten^{-/-}$ mice, T-cell lymphomas originate from $CD4^+CD8^+$ DP thymocytes in the thymus (34, 36).

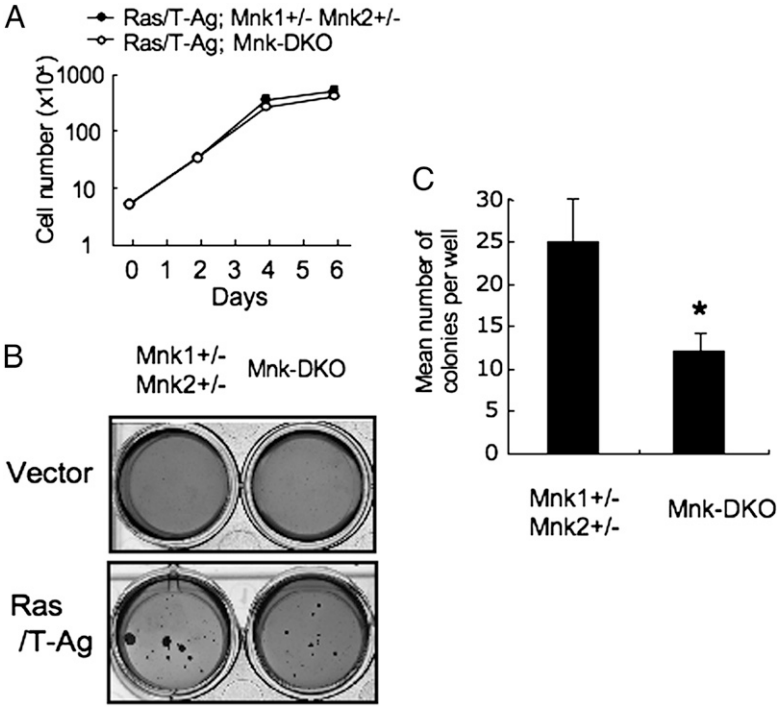

Fig. 2. Primary MEFs from Mnk1$^{-/-}$Mnk2$^{-/-}$ mice are resistant to oncogenic transformation. (*A*) Growth curves under standard conditions. Primary MEFs from mice of the indicated genotypes were infected with H-RasV12 (Ras) plus SV40LT antigen (T-Ag). Transformed cells (5×10^4/well) were plated in six-well plates. (*B* and *C*) Reduced anchorage-independent cell growth. The transformed MEFs of *A* and empty vector-transduced control MEFs were allowed to form colonies for 21 d in soft agar. Colonies were stained with crystal violet (*B*) and colony numbers were counted (*C*). Results shown in *C* are the mean colony number ± SE of triplicate samples and are representative of two independent experiments. *$P = 0.003$ (Student's *t* test).

Before lymphoma development (6 wk of age), the CD4:CD8 profiles of thymocytes from tPten$^{-/-}$; Mnk-DKO and tPten$^{-/-}$; non-Mnk-DKO mice were comparable, suggesting that a lack of Mnk1/2 has no detectable effect on T-lineage cell fate nor on the type of lymphoma developing in the absence of Pten.

Next, we looked at the phosphorylation status of eIF4E in thymic lymphomas from tPten$^{-/-}$; Mnk-DKO and tPten$^{-/-}$; non-Mnk-DKO mice. Significant (but variable) eIF4E phosphorylation was observed in cells isolated from tPten$^{-/-}$; non-Mnk-DKO lymphomas, but none was detectable in cells from tPten$^{-/-}$; Mnk-DKO lymphomas (Fig. 3*D*), indicating that Mnk1/2 kinases are essential for eIF4E phosphorylation in transformed Pten-null cells in vivo. Levels of total eIF4E were variable in lymphoma cells of both genotypes and no consistent differences were observed (Fig. 3*D*). Histological examination showed that, compared with thymocytes from WT C57BL/6 mice, the lymphoma cells in the thymus or spleen of both tPten$^{-/-}$; Mnk-DKO and tPten$^{-/-}$; non-Mnk-DKO mice had scant cytoplasm, enlarged round nuclei, irregular nuclear contours, and prominent nucleoli (Fig. 4 *A–C* and *G–I*), consistent with a previous characterization of tPten$^{-/-}$ lymphoma tissues (35). Immunohistochemical analysis revealed markedly enhanced eIF4E phosphorylation in the perinuclear region of these abnormal cells (Fig. 4 *E* and *K*), but showed that this phosphorylation was abolished in tPten$^{-/-}$; Mnk-DKO lymphoma tissues (Fig. 4 *F* and *L*). These data confirm our immunoblot analyses and indicate that eIF4E phosphorylation via Mnk1/2 may be essential for the promotion of tumor development in this context.

Mnk1 Knockdown Reduces the Tumorigenic Activity of Xenografted U87MG Glioma Cells. Clinical examinations have revealed that Mnk1 is significantly elevated in human glioma tissues (18). Several studies have shown that the potent Mnk inhibitor CGP57380 suppresses human cancer cell growth in vitro (31, 37–39), but it remains unclear whether this inhibition is due to effects on Mnk1/2 or on Mnk1/2 plus other kinases promoting cell growth (40, 41). To investigate the effects of specific Mnk inhibition in the context of human cancer, we set out to use an shRNA-lentivirus system to stably knock down Mnk in human glioma cell lines. We first determined the protein expression levels of Mnk1, Mnk2, and eIF4E in three human glioma cell lines: U87MG, U118MG, and LN-18. U87MG cells, which bear an inactivating mutation of Pten (42), exhibited high levels of Mnk1 protein and strongly enhanced eIF4E phosphorylation but only minimal Mnk2 protein (Fig. S2). This observation suggested that shRNA-mediated knockdown of Mnk1 in the U87MG line would produce cells with a phenotype resembling that of Mnk1/2 double knockdown cells. We therefore infected U87MG cells with lentivirus harboring one of two independent Mnk1 shRNAs, sh#1 or sh#2, that target different sequences of the human Mnk1 gene. Immunoblotting confirmed the successful knockdown of Mnk1 expression in the transduced U87MG cells as well as a substantial reduction in eIF4E phosphorylation (Fig. 5*A*). In addition, Mnk1 knockdown U87MG cells displayed reduced focus formation in culture compared with U87MG cells infected with virus expressing control shRNA (Fig. 5*B*). Last, flow cytometric cell-cycle analysis showed that the S-phase population was significantly reduced in Mnk1 knockdown cells (Fig. 5*C*). Thus, inhibition of Mnk decreases the in vitro oncogenic activity of glioma cells.

To evaluate whether Mnk knockdown cells could form tumors in vivo, we injected U87MG cells expressing Mnk1 sh#1, Mnk1 sh#2, or control shRNA s.c. into NIH III immunodeficient *nude* mice. Whereas the control cells formed tumors in all mice ($n = 10$) by day 30 postinjection, the Mnk1 sh#1-expressing cells did not form detectable tumors in any mouse ($n = 7$) (Student's *t* test, $P = 0.008$; Fisher's exact test, $P = 0.0006$) (Fig. 5 *D* and *E Left*). Injection of U87MG cells expressing Mnk1 sh#2 (a less efficient shRNA) generated tumors in the recipients ($n = 3$), but

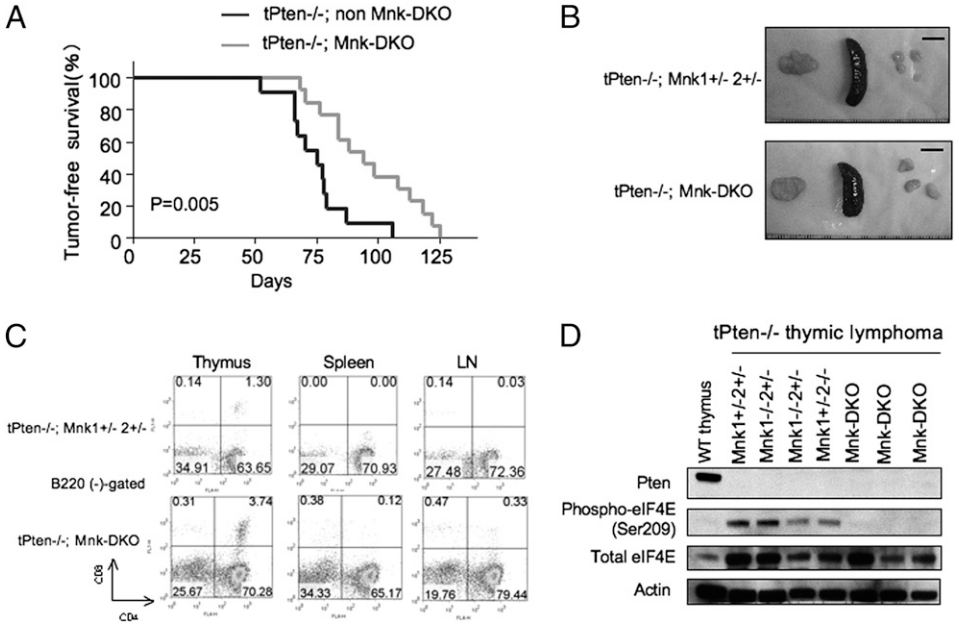

Fig. 3. Combined Mnk1/2 deficiency delays tumorigenesis in T-cell-specific Pten-deficient mice. (*A*) Kaplan–Meier survival plots for tPten$^{-/-}$; Mnk-DKO mice and tPten$^{-/-}$; non-Mnk-DKO (Mnk1$^{+/-}$Mnk2$^{+/-}$, Mnk1$^{-/-}$Mnk2$^{+/-}$, and Mnk1$^{+/-}$Mnk2$^{-/-}$) mice. Mice were killed when tumors measured 1 cm across or at the first signs of mouse morbidity (abdominal distension with hunched back, etc.). Median tumor-free survival: tPten$^{-/-}$; non-Mnk-DKO = 75 d (n = 11; male:female = 5:6), tPten$^{-/-}$; Mnk-DKO = 94 d (n = 13; male:female = 6:7). P = 0.005 (log-rank test). (*B* and *C*) Characterization of tPten$^{-/-}$ T-cell lymphomas. (*B*) Photographs of the thymus, spleen, and lymph nodes (LN) from a representative mouse of the indicated genotypes. Enlarged spleens (splenomegaly; long diameter > 2 cm) were confirmed for all tPten$^{-/-}$ mice in *A*. (Scale bars, 1 cm.) (*C*) Flow cytometric profiles of CD4/CD8 expression by cells isolated from lymphomas in the indicated tissues in *B*. (*D*) Loss of eIF4E phosphorylation in tPten$^{-/-}$; Mnk-DKO lymphomas. WT thymocytes (thymus) and cells isolated from thymic lymphomas in mice of the indicated genotypes were subjected to immunoblotting to detect the indicated proteins. Actin, loading control.

these malignancies were still smaller in size than those arising after injection of control shRNA-expressing cells (Fig. 5 *D* and *E Right*). These results indicate that specific inhibition of Mnk1 (and perhaps also Mnk2) has the potential to suppress human cancer cell growth in vivo.

Discussion

Studies in vivo and in vitro have clearly shown that the Mnk-eIF4E axis promotes transformation and tumor progression (14), a hypothesis also supported by clinical data (13, 15–18). At the mechanistic level, eIF4E overexpression enhances the translation

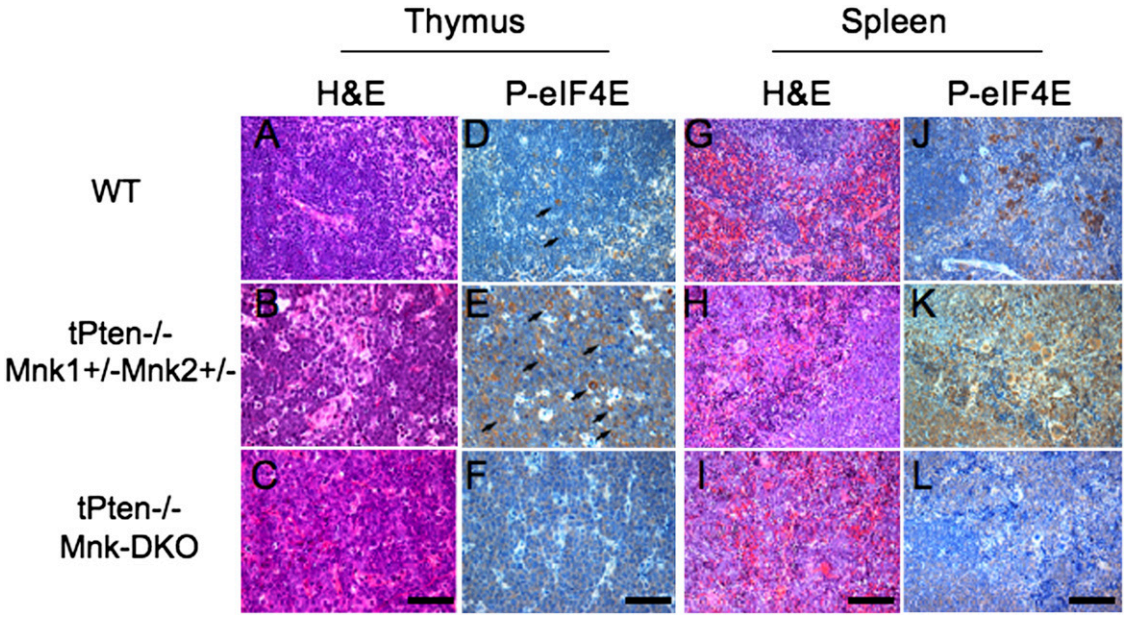

Fig. 4. Combined Mnk1/2 deficiency abolishes eIF4E phosphorylation in lymphomas of T-cell-specific Pten-deficient mice. Sections of WT thymus and spleen and lymphomas from mice of the indicated genotypes were stained with H&E (*A–C* and *G–I*) or with specific antibody to detect phosphorylated eIF4E (P-eIF4E; *D–F* and *J–L*). (Scale bars, 50 μm in *A–F*; 100 μm in *G–L*.) Black arrows, representative phospho-eIF4E^{+} cells.

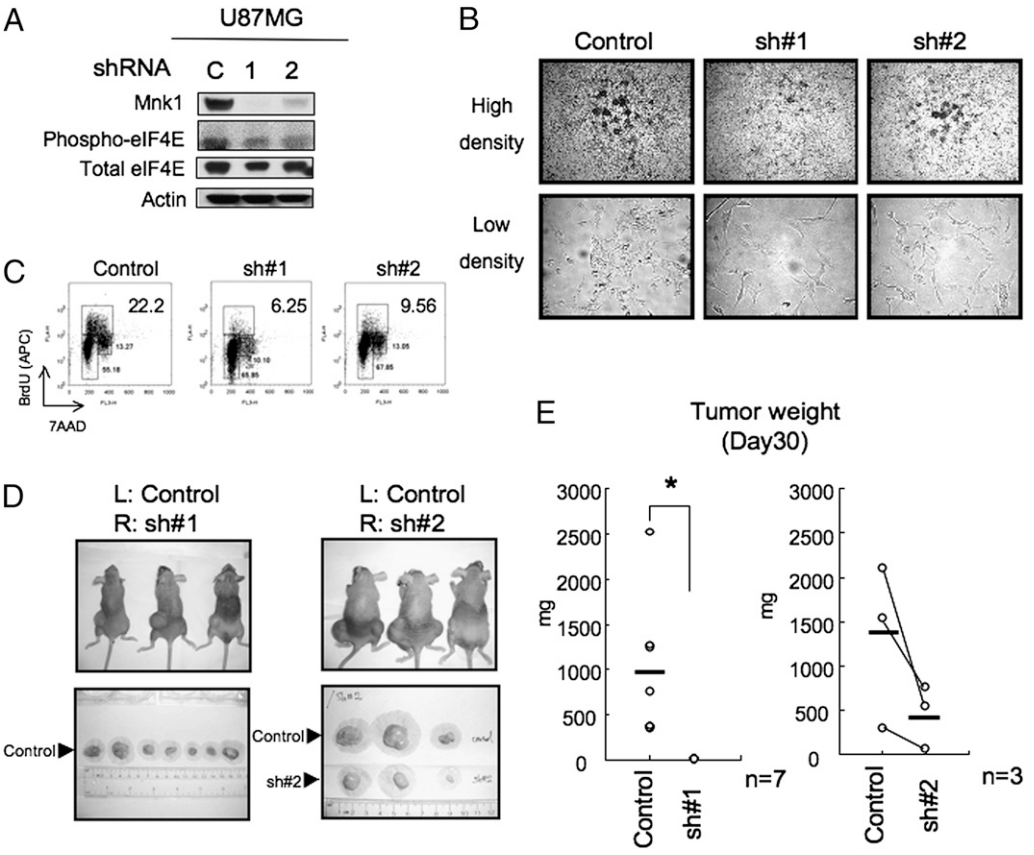

Fig. 5. Mnk1 knockdown reduces tumor growth in a glioma xenograft model. (*A*) Confirmation of Mnk1 knockdown and reduced eIF4E phosphorylation. U87MG cells were infected with virus expressing control shRNA (C), Mnk1 shRNA#1 (1), or Mnk1 shRNA#2 (2). Four days after puromycin selection, lysates were immunoblotted to detect the indicated proteins. (*B*) Reduced focus formation. The cells in *A* were plated at high density (7.5×10^4 cells/well; upper panel) or low density (1×10^4 cells/well; lower panel) and focus formation was examined at 4 or 2 d postplating, respectively. (*C*) Decreased S-phase population. The cells in *A* were seeded at 3×10^5/10-cm plate, cultured for 4 d, and then pulsed with BrdU for 40 min. Cells were stained with APC-anti-BrdU for 20 min to detect BrdU incorporation (vertical axis), and with 7-AAD to detect total DNA content (horizontal axis). Upper box, cells incorporating BrdU (S phase); lower left box, G_0/G_1 cells; lower right box, G_2/M cells; upper right number, percentage of total $BrdU^+$ cells. (*D*) Decreased tumor formation. *Nude* mice were injected with control shRNA-expressing U87MG cells in the left flank (L), and with Mnk1 knockdown cells (either sh#1 or sh#2) in the right flank (R). (*Upper*) Gross appearance of mice. (Lower) Dissected tumors at day 30 postinjection. U87MG cells expressing Mnk1 shRNA#1 did not form detectable tumors. (*E*) Decreased tumor mass. The dissected tumors from *D* were weighed. (*Left*) Each circle represents the tumor mass from one mouse. Horizontal line, mean total mass of all tumors originating from the indicated cells. (*Right*) Weights of control and sh#2-expressing tumors dissected from the same mouse are connected with a line to facilitate comparison. Data from three mice are shown. $^*P$ = 0.008 (Student's *t* test), P = 0.0006 (Fisher's exact test).

of prosurvival genes (43), and inducible eIF4E stimulates the translation of abundant ribosomal protein mRNAs (44). Accordingly, at least in the overexpression setting, the phosphorylation of eIF4E appears to be critical for the translation of the eIF4E target genes that enhance oncogenesis.

In this study, we used a genetically engineered mouse system to show that elevated levels of eIF4E phosphorylation occur in Mnk1/2-expressing, Pten-null lymphomas and that a combined deficiency of Mnk1 and Mnk2 delays lymphoma development in $tPten^{-/-}$ mice. Wang et al. have shown that rapamycin-induced eIF4E phosphorylation mediated by Mnk1/2 is markedly inhibited in PI3K-deficient (p85α; p85β DKO) MEFs (38). This latter result suggests that the Mnk-eIF4E axis is positively regulated not only by the MAP kinase pathway but also by the PI3K pathway, although the mechanism remains to be elucidated. In our study, Pten-null tumors lacking both Mnk1 and Mnk2 exhibited a complete absence of eIF4E phosphorylation, whereas significant (but variable) eIF4E phosphorylation was seen in Pten-null tumors expressing either Mnk1 or Mnk2. Thus, Mnk1/2-mediated eIF4E phosphorylation enhances the tumorigenesis associated with loss of Pten. To date, no obvious differences in tumor development have been observed among Pten-null mice that expressed at least one Mnk enzyme, suggesting that these malignancies depend solely on the presence of some level of elevated eIF4E phosphorylation. At this time, however, we cannot rule out the possibility that our observations may also be partly due to the effect of Mnk activities on other known substrates such as Sprouty2, cPLA2, and hnRNPA1 (22–25). These substrates are reportedly involved in cell growth or tumorigenesis (45–48), but the in vivo significance of their phosphorylated forms has yet to be proven.

Our findings in cultured cells support our in vivo results. Primary Mnk-DKO fibroblasts were resistant to Ras-mediated transformation, and stable knockdown of Mnk1 in U87MG human glioma cells, in which Mnk2 expression is very low, significantly retarded tumor formation in NIH III *nude* mice. These data not only show that Mnk1/2 kinases influence tumorigenic events but also suggest that inhibitors of Mnk1/2 may be effective anticancer drugs, particularly for tumors exhibiting mutated, nonfunctional Pten. Moreover, because Mnk1/2 kinases are dispensable for cell growth and embryogenesis, such inhibitory drugs are likely to have minimal side effects.

The mechanism underlying Mnk1/2's oncogenic influence remains unclear. Akt is a critical tumor accelerator that acts down-

stream of the Pten-PI3K pathway but upstream of eIF4E (9, 12). We confirmed that total Akt levels and the Akt phosphorylation induced by IGF-1 or EGF were comparable in Mnk-DKO and control MEFs (Fig. S3), indicating that other critical effectors likely exist downstream of Mnk1/2. The search for these effectors will no doubt contribute to elucidating the mechanism by which Mnk1/2 kinases promote cancer development, and may lead to the discovery of effective and specific drugs targeting the Mnk1/2 pathway.

Materials and Methods

Mice. $Mnk1^{-/-}Mnk2^{-/-}$ mice and $LckCrePten^{flox/flox}$ ($tPten^{-/-}$) mice have been previously described (7, 35). The original strains were derived from R1(129/sv) or E14K (129/Ola) embryonic stem cells. All mice used for experiments in this study were backcrossed more than six times to the C57B/6N or C57B/6J background. All $tPten^{-/-}$; non-Mnk-DKO ($Mnk1^{+/-}Mnk2^{+/-}$, $Mnk1^{-/-}Mnk2^{+/-}$, and $Mnk1^{+/-}Mnk2^{-/-}$) mice and most $tPten^{-/-}$; Mnk-DKO mice were generated by breeding the above backcrossed mice. Some $tPten^{-/-}$; Mnk-DKO mice were generated by crossing $LckCrePten^{flox/+}Mnk1^{-/-}Mnk2^{-/-}$ and $Pten^{flox/flox}Mnk1^{-/-}Mnk2^{-/-}$ mice. All animals were treated in accordance with the National Institutes of Health Guide for Care and Use of Laboratory Animals as approved by the University Health Network Animal Care Committee (Toronto, ON, Canada).

Cells, Cell Lines, and Standard Culture Conditions. Primary MEFs were prepared from day 13.5 mouse littermate embryos as previously described (7). For standard culture conditions, primary MEFs [passage (P) 2 or P3] were cultured in Dulbecco's modified Eagle medium (DMEM) with 10% fetal calf serum (FCS). Cells from mouse thymus, spleen, and lymph nodes were isolated using standard protocols. The human glioma cell lines U87MG, U118MG, and LN-18 were from the American Type Culture Collection. U87MG and U118MG cells were cultured in DMEM with 10% FCS, and LN-18 cells were cultured in DMEM with 5% FCS.

Stress Culture Conditions. For L-glutamine starvation, primary MEFs were cultured in L-glutamine-free DMEM with 10% dialyzed FCS and supplemented with 0, 0.4, or 2 mM L-glutamine (GIBCO). For glucose starvation, primary MEFs were cultured in D-glucose-free DMEM with 10% dialyzed FCS. For hypoxia, spontaneously immortalized MEFs derived as described (30) were cultured for 24 h in 0.2% oxygen in an Invivo2 Hypoxia Workstation 400 (Biotrace). For ROS determinations, spontaneously immortalized MEFs were treated with H_2O_2 for 30 min at the concentrations indicated in Fig. S1. ROS levels were detected as described in the Fig. S1 legend.

Real-Time RT-PCR Quantification of mRNA. Total RNA was extracted and purified using the RNeasy kit (QIAGEN) according to the manufacturer's protocol. Purified RNA was treated with DNaseI and reverse-transcribed using the SuperScript first-strand RT-PCR kit (Invitrogen); cDNAs were subjected to quantitative real-time PCR using the SYBR Green PCR Master Mix. Primer sequences were as follows: murine Glut1: 5′-AGAGGTGTCACCTACAGCTC-3′, 5′-AACAGGATACACTGTAGCAG-3′; murine Vegf: 5′-TACTGCCGTCCGATTGAGAC-3′, 5′-TGATCTGCATGGTGATGTTG-3′; murine β-actin: 5′-TGTGATGGTGGGAATGGGTCAG-3′, 5′-TTTGATGTCACGCACGATTTCC-3′.

Ras-Mediated Transformation of Primary MEFs and Soft Agar Assays. The Phoenix packaging cell line was used for the generation of ecotropic viruses. MEFs were transduced with the SV40LT and H-RasV12 oncogenes using retroviral infection of the pBabe-puro-SV40LT plus pBabe-hygro-H-RasV12, pBabe-puro, or pBabe-hygro vectors. Transduced cells were selected by growth first in puromycin (2 μg/mL; Sigma) for 3 d and then in hygromycin (200 μg/mL; Invitrogen) for 6 d. Soft agar assays were performed as described (49) with minor modifications. Selected cells were plated at 5×10^3 cells/well of a 12-well plate and allowed to form colonies for 21 d before staining with 0.002% crystal violet dye (Sigma) in PBS. Visible stained colonies were counted.

Production of shRNA-Expressing Lentivirus and Generation of Stable shRNA-Expressing Cell Lines. Human Mnk1 shRNA constructs RHS4430-98853157 (sh#1) and RHS4430-98485774 (sh#2) cloned into pGIPZ lentiviral shRNAmir, and the control shRNA construct (nonsilencing-GIPZ lentiviral shRNAmir control RHS4346), were purchased from Open Biosystems. Lentivirus preparations were made using a three-plasmid packaging system as previously described (50) with some modifications. Briefly, shRNAs in the pGIPZ vector were cotransfected into 293T cells along with expression vectors containing the gag/pol, rev, and vsvg genes. The medium was changed 24 h after transfection. Lentivirus supernatant was harvested 48 h after transfection and diluted 10-fold, followed by the addition of 8 μg/mL polybrene (Sigma-Aldrich).

For stable cell-line generation, U87MG glioma cells were plated at 1×10^5 cells/well in six-well plates and infected for 24 h. Infected cells were selected in 1.5 μg/mL puromycin for 4 d followed by culture in medium containing 1 μg/mL puromycin. Puromycin was removed by washing before cells were plated for experiments.

Tumor Formation in Xenografted Mice. Female NIH III *nude* mice (8-wk-old; Charles River) were injected s.c. into the left or right flank with 1×10^6 control shRNA-expressing or Mnk1 shRNA-expressing U87MG glioma cells, respectively. Tumor formation was assessed by inspection every 2–3 d. On day 30 postinjection, tumors were isolated by dissection and weighed.

Proliferation and Apoptosis Assays. For cell-cycle analyses, BrdU incorporation was assessed using the APC BrdU Flow Kit (BD Pharmingen) and flow cytometry according to the manufacturer's protocols. Cell-death analysis was performed by flow cytometry using propidium iodide (PI) staining together with Annexin V-APC (BD Pharmingen).

Flow Cytometric Analyses. Cells from thymus, spleen, and lymph nodes were stained with the following antibodies: anti-CD4-APC (RM4.5), anti-CD8-FITC (53-6.7), and anti-B220/CD45R (RA3-6B2)-PE (all from BD Biosciences). All flow cytometric data were acquired using a FACSCalibur (Becton-Dickinson) and analyzed with FlowJo software (Tree Star).

Immunoblotting. Antibodies used for immunoblotting were: anti-phospho-eIF4E (Ser209), anti-total eIF4E, anti-total Akt, and anti-phospho-Akt (Ser473) (all from Cell Signaling); anti-Mnk2 (S-20) (Santa Cruz Biotechnology); anti-human PTEN (6H2.1) (Cascade Biosciences); and anti-β-actin (Sigma). Standard lysate preparation and electroblotting protocols were used.

Histology. Tissue samples were fixed in 10% buffered formalin at room temperature and embedded in paraffin. Sections (5-μm) were stained with hematoxylin and eosin (H&E) according to standard protocols. Immunohistochemistry to detect the phospho-eIF4E signal required microwave antigen retrieval in sodium citrate buffer (pH 6) performed using a standard protocol (51). Anti-phospho-eIF4E (Ser209) (Cell Signaling) was used at 1:32 as the primary antibody, and biotinylated goat anti-rabbit IgG (Jackson ImmunoResearch Laboratories) was used as the secondary antibody. An ABC kit (Vector Labs; 1.5 h) and diaminobenzidine were used to develop the signal. Sections were lightly counterstained with hematoxylin.

Statistics. Mouse survival curves were constructed using Kaplan–Meier methodology and compared by the log-rank test using GraphPad Prism software. Other statistical analyses were performed using the Student's *t* test unless otherwise stated.

ACKNOWLEDGMENTS. We thank N. Sonenberg, H. Kuwata, and M. Kawazu for helpful discussions, and M. Saunders for scientific editing. This work was supported by a grant from the Canadian Institute of Health Research (to T.W.M.).

1. Fukunaga R, Hunter T (1997) MNK1, a new MAP kinase-activated protein kinase, isolated by a novel expression screening method for identifying protein kinase substrates. *EMBO J* 16:1921–1933.
2. Waskiewicz AJ, Flynn A, Proud CG, Cooper JA (1997) Mitogen-activated protein kinases activate the serine/threonine kinases Mnk1 and Mnk2. *EMBO J* 16:1909–1920.
3. Waskiewicz AJ, et al. (1999) Phosphorylation of the cap-binding protein eukaryotic translation initiation factor 4E by protein kinase Mnk1 in vivo. *Mol Cell Biol* 19:1871–1880.
4. Pyronnet S, et al. (1999) Human eukaryotic translation initiation factor 4G (eIF4G) recruits Mnk1 to phosphorylate eIF4E. *EMBO J* 18:270–279.
5. Pyronnet S (2000) Phosphorylation of the cap-binding protein eIF4E by the MAPK-activated protein kinase Mnk1. *Biochem Pharmacol* 60:1237–1243.
6. Gingras AC, Raught B, Sonenberg N (1999) eIF4 initiation factors: Effectors of mRNA recruitment to ribosomes and regulators of translation. *Annu Rev Biochem* 68: 913–963.
7. Ueda T, Watanabe-Fukunaga R, Fukuyama H, Nagata S, Fukunaga R (2004) Mnk2 and Mnk1 are essential for constitutive and inducible phosphorylation of eukaryotic initiation factor 4E but not for cell growth or development. *Mol Cell Biol* 24: 6539–6549.

8. Mamane Y, et al. (2004) eIF4E—From translation to transformation. *Oncogene* 23: 3172–3179.
9. Wendel HG, et al. (2004) Survival signalling by Akt and eIF4E in oncogenesis and cancer therapy. *Nature* 428:332–337.
10. Cully M, You H, Levine AJ, Mak TW (2006) Beyond PTEN mutations: The PI3K pathway as an integrator of multiple inputs during tumorigenesis. *Nat Rev Cancer* 6:184–192.
11. Graff JR, et al. (2009) eIF4E activation is commonly elevated in advanced human prostate cancers and significantly related to reduced patient survival. *Cancer Res* 69: 3866–3873.
12. Ruggero D, et al. (2004) The translation factor eIF-4E promotes tumor formation and cooperates with c-Myc in lymphomagenesis. *Nat Med* 10:484–486.
13. Fan S, et al. (2009) Phosphorylated eukaryotic translation initiation factor 4 (eIF4E) is elevated in human cancer tissues. *Cancer Biol Ther* 8:1463–1469.
14. Wendel HG, et al. (2007) Dissecting eIF4E action in tumorigenesis. *Genes Dev* 21: 3232–3237.
15. Yoshizawa A, et al. (2010) Overexpression of phospho-eIF4E is associated with survival through AKT pathway in non-small cell lung cancer. *Clin Cancer Res* 16:240–248.
16. Pellagatti A, et al. (2003) Gene expression profiling in polycythemia vera using cDNA microarray technology. *Cancer Res* 63:3940–3944.
17. Worch J, et al. (2004) The serine-threonine kinase MNK1 is post-translationally stabilized by PML-RARα and regulates differentiation of hematopoietic cells. *Oncogene* 23: 9162–9172.
18. Bredel M, et al. (2005) High-resolution genome-wide mapping of genetic alterations in human glial brain tumors. *Cancer Res* 65:4088–4096.
19. Hendrix ND, et al. (2006) Fibroblast growth factor 9 has oncogenic activity and is a downstream target of Wnt signaling in ovarian endometrioid adenocarcinomas. *Cancer Res* 66:1354–1362.
20. Lazaris-Karatzas A, Montine KS, Sonenberg N (1990) Malignant transformation by a eukaryotic initiation factor subunit that binds to mRNA 5′ cap. *Nature* 345:544–547.
21. Topisirovic I, Ruiz-Gutierrez M, Borden KL (2004) Phosphorylation of the eukaryotic translation initiation factor eIF4E contributes to its transformation and mRNA transport activities. *Cancer Res* 64:8639–8642.
22. Hefner Y, et al. (2000) Serine 727 phosphorylation and activation of cytosolic phospholipase A2 by MNK1-related protein kinases. *J Biol Chem* 275:37542–37551.
23. DaSilva J, Xu L, Kim HJ, Miller WT, Bar-Sagi D (2006) Regulation of Sprouty stability by Mnk1-dependent phosphorylation. *Mol Cell Biol* 26:1898–1907.
24. Guil S, Long JC, Cáceres JF (2006) hnRNP A1 relocalization to the stress granules reflects a role in the stress response. *Mol Cell Biol* 26:5744–5758.
25. Buxadé M, et al. (2005) The Mnks are novel components in the control of TNF α biosynthesis and phosphorylate and regulate hnRNP A1. *Immunity* 23:177–189.
26. Bert AG, Grépin R, Vadas MA, Goodall GJ (2006) Assessing IRES activity in the HIF-1α and other cellular 5′ UTRs. *RNA* 12:1074–1083.
27. Semenza GL (2003) Targeting HIF-1 for cancer therapy. *Nat Rev Cancer* 3:721–732.
28. Svitkin YV, et al. (2005) Eukaryotic translation initiation factor 4E availability controls the switch between cap-dependent and internal ribosomal entry site-mediated translation. *Mol Cell Biol* 25:10556–10565.
29. Koumenis C, Wouters BG (2006) "Translating" tumor hypoxia: Unfolded protein response (UPR)-dependent and UPR-independent pathways. *Mol Cancer Res* 4:423–436.
30. Chrestensen CA, et al. (2007) Loss of MNK function sensitizes fibroblasts to serum-withdrawal induced apoptosis. *Genes Cells* 12:1133–1140.
31. Origanti S, Shantz LM (2007) Ras transformation of RIE-1 cells activates cap-independent translation of ornithine decarboxylase: Regulation by the Raf/MEK/ERK and phosphatidylinositol 3-kinase pathways. *Cancer Res* 67:4834–4842.
32. Gupta S, et al. (2007) Binding of Ras to phosphoinositide 3-kinase p110α is required for Ras-driven tumorigenesis in mice. *Cell* 129:957–968.
33. Cully M, et al. (2004) grb2 heterozygosity rescues embryonic lethality but not tumorigenesis in pten$^{+/-}$ mice. *Proc Natl Acad Sci USA* 101:15358–15363.
34. Xue L, Nolla H, Suzuki A, Mak TW, Winoto A (2008) Normal development is an integral part of tumorigenesis in T cell-specific PTEN-deficient mice. *Proc Natl Acad Sci USA* 105:2022–2027.
35. Suzuki A, et al. (2001) T cell-specific loss of Pten leads to defects in central and peripheral tolerance. *Immunity* 14:523–534.
36. Hagenbeek TJ, Spits H (2008) T-cell lymphomas in T-cell-specific Pten-deficient mice originate in the thymus. *Leukemia* 22:608–619.
37. Chrestensen CA, et al. (2007) MNK1 and MNK2 regulation in HER2-overexpressing breast cancer lines. *J Biol Chem* 282:4243–4252.
38. Wang X, et al. (2007) Inhibition of mammalian target of rapamycin induces phosphatidylinositol 3-kinase-dependent and Mnk-mediated eukaryotic translation initiation factor 4E phosphorylation. *Mol Cell Biol* 27:7405–7413.
39. Bianchini A, et al. (2008) Phosphorylation of eIF4E by MNKs supports protein synthesis, cell cycle progression and proliferation in prostate cancer cells. *Carcinogenesis* 29: 2279–2288.
40. Zhang M, et al. (2008) Inhibition of polysome assembly enhances imatinib activity against chronic myelogenous leukemia and overcomes imatinib resistance. *Mol Cell Biol* 28:6496–6509.
41. Bain J, et al. (2007) The selectivity of protein kinase inhibitors: A further update. *Biochem J* 408:297–315.
42. Ishii N, et al. (1999) Frequent co-alterations of TP53, p16/CDKN2A, p14ARF, PTEN tumor suppressor genes in human glioma cell lines. *Brain Pathol* 9:469–479.
43. Larsson O, et al. (2006) Apoptosis resistance downstream of eIF4E: Posttranscriptional activation of an anti-apoptotic transcript carrying a consensus hairpin structure. *Nucleic Acids Res* 34:4375–4386.
44. Mamane Y, et al. (2007) Epigenetic activation of a subset of mRNAs by eIF4E explains its effects on cell proliferation. *PLoS One* 2:e242.
45. Edwin F, Anderson K, Patel TB (2010) HECT domain-containing E3 ubiquitin ligase Nedd4 interacts with and ubiquitinates Sprouty2. *J Biol Chem* 285:255–264.
46. Panel V, et al. (2006) Cytoplasmic phospholipase A2 expression in human colon adenocarcinoma is correlated with cyclooxygenase-2 expression and contributes to prostaglandin E2 production. *Cancer Lett* 243:255–263.
47. Karni R, et al. (2007) The gene encoding the splicing factor SF2/ASF is a proto-oncogene. *Nat Struct Mol Biol* 14:185–193.
48. David CJ, Chen M, Assanah M, Canoll P, Manley JL (2010) HnRNP proteins controlled by c-Myc deregulate pyruvate kinase mRNA splicing in cancer. *Nature* 463:364–368.
49. Maeda T, et al. (2005) Role of the proto-oncogene Pokemon in cellular transformation and ARF repression. *Nature* 433:278–285.
50. Root DE, Hacohen N, Hahn WC, Lander ES, Sabatini DM (2006) Genome-scale loss-of-function screening with a lentiviral RNAi library. *Nat Methods* 3:715–719.
51. Kanungo AK, Hao Z, Elia AJ, Mak TW, Henderson JT (2008) Inhibition of apoptosome activation protects injured motor neurons from cell death. *J Biol Chem* 283:22105–22112.